Letter

Contact-mediated signaling enables disorder-driven transitions in cellular assemblies

Chandrashekar Kuyyamudi,[1,2] Shakti N. Menon,[1] and Sitabhra Sinha[1,2]
[1]*The Institute of Mathematical Sciences, CIT Campus, Taramani, Chennai 600113, India*
[2]*Homi Bhabha National Institute, Training School Complex, Anushaktinagar, Mumbai 400 094, India*

(Received 22 February 2022; accepted 2 August 2022; published 22 August 2022)

We show that, when cells communicate by contact-mediated interactions, heterogeneity in cell shapes and sizes leads to qualitatively distinct collective behavior in the tissue. For intercellular coupling that implements lateral inhibition, such disorder-driven transitions can substantially alter the asymptotic pattern of differentiated cells by modulating their fate choice through changes in the neighborhood geometry. In addition, when contact-induced signals influence inherent cellular oscillations, disorder leads to the emergence of functionally relevant partially-ordered dynamical states.

DOI: 10.1103/PhysRevE.106.L022401

Many natural systems, ranging from granular materials to biological tissues and dense crowds, are characterized by varying levels of heterogeneity in their structural attributes [1–7]. This disorder arises via self-organization as a result of interactions between their numerous constituent units, causing their arrangement to deviate from regular lattice ordering [8–11]. A striking example is provided by confluent epithelial tissue, wherein cells are packed together in a high state of disorder characterized by quantitative measures that incorporate the area, perimeter, or number of neighbors of each cell [12–14]. As such cells communicate with each other, e.g., via the ubiquitous Notch pathway in which signaling occurs through receptor-ligand binding [15–17], disorder can have remarkable functional consequences. Note that the Notch pathway effectively implements *lateral inhibition* through which the induction of a specific fate in a cell prevents its immediate neighbors from expressing the same fate [18,19]. As this is one of the principal mechanisms for tissue patterning [20,21], disordered contact geometry, which alters the nature of interactions between adjacent cells, can affect their fates [22]. An important question in this context concerns the relative roles of local, contact-mediated interactions and global forces that alter the degree of disorder in shaping the collective behavior of cellular assemblies.

Such interplay between disorder and interactions is strikingly apparent during the appearance of a characteristic spatial pattern in the basal papilla (the auditory sensory organ in all amniotes [23]) comprising specialized sensory "hair cells" that are separated from each other by intervening support cells [Fig. 1(a)]. As either cell type can arise from the same progenitor cell, the specific fate induced in a particular cell depends on the cues it receives from its neighborhood [24]. In particular, hair cells inhibit their immediate neighbors from adopting the same fate [18,25]. Disorder in the cellular arrangement can drastically affect these cues and, consequently, the resulting fate choice. More generally, one can investigate novel qualitative features in the collective behavior, such as partially ordered or "chimera" states [26,27], that may result from structural heterogeneities. This is particularly relevant where heterogeneity arises through flexibility in cell shapes, typically observed at the embryonic stage [28] but retained lifelong in simpler animals such as *Trichoplax adhaerens* [29]. The resulting disordered arrangement of cells in this organism, when coupled to the oscillatory dynamics of the cilia of each cell, can affect organism-level behavior such as gliding locomotion propelled by collective beating of the cilia [30,31] [Fig. 1(b)]. These examples suggest that the composition and function of tissues can be altered significantly with increasing heterogeneity in cell sizes and shapes.

In this Letter we explicitly demonstrate such transitions with increasing disorder in the arrangement of cells that interact via contact-induced signaling. When the interactions between cells implement lateral inhibition, it can influence fate induction to alter the relative proportions of distinct cell types, and consequently affect development. We also demonstrate that in tissues where cells are susceptible to random failures in their ability to communicate with neighbors, heterogeneity in the cellular packing geometry makes the asymptotic pattern of differentiated cells more robust. Further, we show that, if the intercellular interactions modulate cell activity such as oscillations in molecular concentrations [32–35], disorder promotes the emergence of chimera states. These are characterized by the coexistence of oscillating cells with those whose activity has been arrested, and we show that they arise irrespective of whether cells are coupled through receptor-ligand binding or by diffusion across bridges such as gap junctions [Fig. 1(c)–1(e)]. Thus, selective deformation of a cellular assembly can drive transitions between dynamical states marked by different proportions of oscillating elements, suggesting an intriguing locomotory mechanism in simple multicellular organisms.

To generate disordered cellular configurations, we use Voronoi tessellations to construct two-dimensional space-filling tilings with nonoverlapping polygons, characterized by varying levels of heterogeneity. We introduce disorder in a regular hexagonal lattice by adding Gaussian noise $\mathcal{N}(0, \sigma_P)$ to randomly displace each of the generating points or seeds (initially, the centroids of the hexagons). The standard

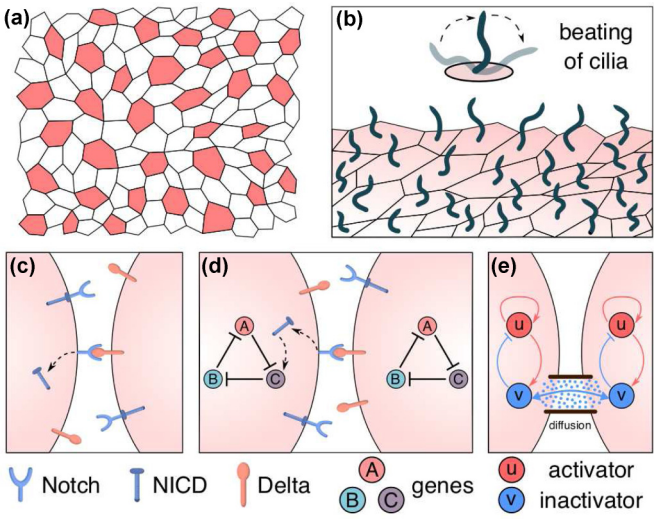

FIG. 1. Communication between neighboring cells in a closepacked disordered configuration underlie a range of collective behavior. (a) Schematic diagram of the spatial arrangement of hair cells (shown in red) surrounded by supporting cells in the avian basilar papilla, at an early stage of development [24]. (b) Ventral tissue of the marine animal *Trichoplax adhaerens* illustrated schematically to show the arrangement of monociliated epithelial cells [36–38]. Each of the cilia engage in periodic motion ("beating," see inset) that helps propel the organism across a surface [30,31]. (c)–(e) The key qualitative features of the collective dynamics in such systems are seen to be invariant despite differences in the means by which cells communicate and the dynamics within each cell, e.g., in cells coupled via *trans*-activation of Notch receptors by Delta ligands resulting in release of a downstream effector (NICD) [shown in (c)], repressilators coupled by Notch-Delta signaling (d) and relaxation oscillators coupled via diffusion of the inactivation variable through intercellular bridges such as gap junctions (e).

deviation σ_P can be tuned to yield different levels of heterogeneity. The extent of disorder in the lattice, measured by the variance $\sigma^2(l_e)$ of the perimeters of the cellular polygons, reaches its maximal value for $\sigma_P \sim 1$ and does not change appreciably on increasing σ_P further (Fig. 2). The coupling strength between a pair of adjacent cells is assumed to be proportional to the total interface length. A weighted adjacency matrix $\mathbf{A}$, with A_{ij} representing the overlap between the cells i and j, thus provides the information required to assign interaction strengths between each pair of cells.

We consider contact-induced signaling via Notch receptors located on the surface of a cell binding to ligands (e.g., Delta) embedded on the membrane of a neighboring cell (i.e., *trans* binding). This is represented by the following set of equations describing the time-evolutions of the concentrations of the receptor (R), ligand (L), and the Notch intra-cellular domain or NICD (S), the downstream effector of the Notch signaling pathway:

$$\frac{dR_i}{dt} = \beta_R - \gamma_R R_i - k_{cis} R_i L_i - k_{tr} R_i L_i^{tr}, \tag{1}$$

$$\frac{dL_i}{dt} = \frac{\beta_L K_s^h}{K_s^h + S_i^h} - \gamma_L L_i - k_{cis} R_i L_i - k_{tr} L_i R_i^{tr}, \tag{2}$$

$$\frac{dS_i}{dt} = k_{tr} R_i L_i^{tr} - \gamma_S S_i. \tag{3}$$

Here $R_i^{tr} = \sum_j A_{ij} R_j$ and $L_i^{tr} = \sum_j A_{ij} L_j$ are the weighted sums of receptor and ligand concentrations, respectively, in the neighborhood of the ith cell. Earlier studies have shown that lateral inhibition requires strong inhibition of Notch receptors via *cis* binding (i.e., to ligands on the same cell) [18,19]. Consistent with this, we choose $k_{tr} = 0.13$ and $k_{cis} = 4.64$, which are related to the rates of *trans* activation and *cis* inhibition, respectively. The maximal production rates of both receptors (β_R) and ligands (β_D) are chosen to be 100. The contact-induced signal is assumed to have a relatively longer lifetime so that the degradation rates of the receptors (γ_R), ligands (γ_D), and NICD (γ_S) are chosen as 1, 1, and 0.1, respectively. The repression of ligand production by the downstream effector of Notch signaling pathway is modeled by a Hill function, parametrized by $K_s(=10)$ and $h(=4)$. The initial concentrations for the ligands and receptors are chosen from a uniform random distribution defined over the domain [0,10]. In the presence of strong *cis* inhibition, only those cells in which ligands far outnumber receptors can engage in *trans* activation of Notch receptors of neighboring cells. Consequently, the production of ligands in these cells is inhibited [see Eq. (2)]. The resulting unequal distribution of ligands among cells results in each cell eventually becoming either (i) a *receiver* for contact-induced intercellular signals, having receptors but no ligands, or (ii) a *transmitter* of signals, possessing ligands but no receptors. Mutual competition for *trans*-binding between neighboring cells having more ligands than receptors is reinforced by the suppression of ligand production in the cell whose receptors are activated. Thus, each cell which develops into a transmitter would be surrounded exclusively by cells that become receivers [18]. This mutual "repulsion" between transmitters imposes a strong constraint on their numbers as such cells need to be separated from each other by receiver cells. For example, this requirement would allow only $\sim N/3$ transmitters in a hexagonal lattice comprising N cells. However, if we instead consider a disordered arrangement of cells, the total number of transmitters allowed increases noticeably. This can be seen from the steady-state patterns of cellular ligand concentration L_{SS} as σ_P is increased [Fig. 2(a)]. Note that this phenomenon can be observed independent of the specific pattern in which low and high values of L_{SS} occur across the cellular array. In particular, the increase in transmitter cells would arise even if the low and high L_{SS} states are arranged in a periodic, spatially regular pattern (such as those described in Refs. [39,40]). This can be demonstrated explicitly by locally deforming the geometry of cellular arrangement in a specific neighborhood so as to isolate one of the receiver cells from its neighboring transmitter cells, thereby allowing it to become a transmitter cell itself (augmenting their number by unity) [41].

The observed bimodal nature of the L_{SS} distribution, which is invariant to the degree of disorder [Fig. 2(b)], allows a natural segregation of the cells into receivers (lower peak) and transmitters (higher peak). Further, we note that the cell-cell interface lengths (l_c), which crucially dictate the magnitude of the contact-induced signal, exhibit higher variance with increased disorder [Fig. 2(c)]. This is mirrored in the rise of the number of transmitter cells n_h with σ_P [Fig. 2(c)]. The broadening of the peaks in the L_{SS} distribution with increasing heterogeneity can be understood in terms of the role that the

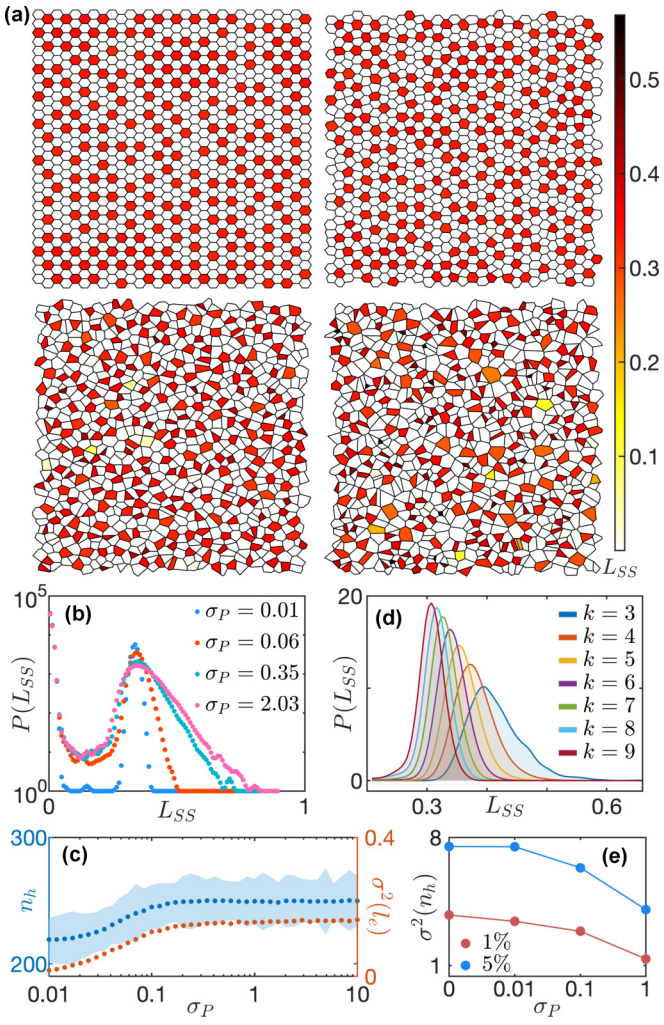

FIG. 2. Higher disorder in the cellular packing configuration allows a more equitable and robust distribution of cell fates. (a) Spatial patterns formed by the steady state Delta ligand concentration, L_{SS} (see color bar) in an assembly of $N(=900)$ cells resulting from lateral inhibition. The panels show lattices with increasing structural disorder, as indicated by the dispersion of the deviations in cell positions from those in the regular hexagonal lattice: $\sigma_P = 0$ (top left), 0.01 (top right), 0.1 (bottom left), and 1 (bottom right). As seen from the bimodal distribution in (b), cells either have very low or high values of L_{SS}. The increase in the width of the high L_{SS} peak with disorder is quantified in (c) which shows that the number of cells n_h (blue dots) in this state, i.e., cells having $L_{SS} > 0.2$, increases with the disorder. We have verified that the specific choice of the threshold value does not qualitatively change our results. The shaded region represents the dispersion in n_h. The variance of the cell perimeters [$\sigma^2(l_c)$, red dots] also rises with disorder in a qualitatively similar manner. (d) The asymptotic ligand concentration in a cell appears to be correlated with the number of its neighbors k. The L_{SS} distributions in cells with a specific k monotonically shift to left with increasing k, suggesting that cells in states characterized by higher L_{SS} have fewer neighbors than average. (e) Greater robustness to damage in the cellular array is seen with increased disorder, as evident from the reduced variability of fate distribution (measured in terms of dispersion in n_h) with rise in σ_P when 1% (red) or 5% (blue) of randomly chosen cells are rendered inert.

degree k of a transmitter cell (i.e., the number of cells in its immediate neighborhood) plays in determining the steady state ligand concentration. Figure 2(d) shows that the ligand distribution of cells having exactly k neighbors shifts to the right with decreasing k. Thus, the peakbroadening with σ_P [Fig. 2(b)] can be attributed to a higher density of transmitter cells with lower k (compared to the regular lattice). With increasing heterogeneity, transmitter cells have fewer neighbors on average, implying that more cells can become transmitters as their number is only limited by the constraint that no two of them can be neighbors.

As transmitters and receivers correspond to cells with distinct fates, any change in their relative proportions resulting from disordered cellular arrangements may alter the course of development. Heterogeneity also makes the spatial pattern robust against damage that may strike a cell at random, disabling it from taking part in inter-cellular signaling [41]. This is quantified by the dispersion in n_h, the number of cells likely to become transmitters, shown in Fig. 2(e) for two different fractions of randomly damaged cells. As σ_P is increased, the variance decreases noticeably, suggesting that more disordered cellular configurations have less variability in terms of the relative proportion of cells having distinct fates.

The model system reported above focuses only on signaling between cells, without considering how it can alter intra-cellular dynamics. However, Notch signaling plays an important role in processes such as somitogenesis [42,43] and tissue growth by cell division [44,45], where it mediates nontrivial dynamics involving periodically varying molecular concentrations. Therefore, we now consider cellular dynamics described by an oscillating circuit comprising three cyclically repressing genes A, B, and C [46], one of which is chosen to be regulated by the intercellular signal S. The collective dynamics of these cellular oscillators coupled by Notch signaling (specifically, by S inhibiting C) can be described by the time evolution of R, L, and S described earlier (with $h = 2$, other parameter values unchanged), augmented by the following equations for the gene products:

$$\frac{dA_i}{dt} = \alpha\left[\frac{K^g}{K^g + C_i^g}\right] - \frac{A_i}{\tau},$$

$$\frac{dB_i}{dt} = \alpha\left[\frac{K^g}{K^g + A_i^g}\right] - \frac{B_i}{\tau},$$

$$\frac{dC_i}{dt} = \alpha\left[\frac{K^g}{K^g + B_i^g}\right]\left[\frac{Q^g}{Q^g + S_i^g}\right] - \frac{C_i}{\tau}.$$

The maximal production rates $\alpha(=10)$, mean lifetimes $\tau(=1)$, and the parameters $K(=1)$ and $g(=4)$ of the Hill functions describing the cyclic repression are chosen to ensure oscillations in absence of inter-cellular coupling. The repression of gene expression by S is also modeled by a Hill function, parametrized by the exponent $g(=4)$ and the half-saturation constant Q. Upon strengthening the repression (i.e., increasing $1/Q$), the collective dynamics shows a transition from global oscillations to a quiescent state via oscillation arrest.

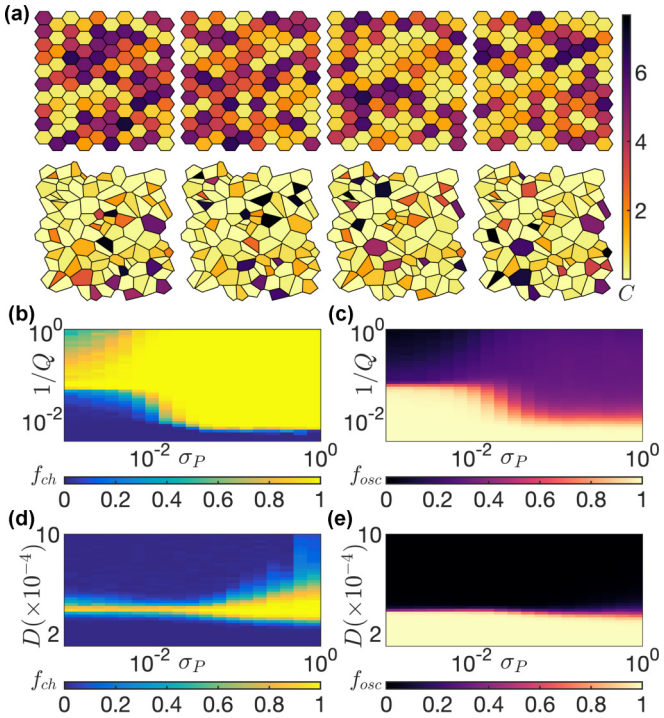

FIG. 3. Disorder promotes the coexistence of qualitatively distinct behaviors (chimera states) in the collective dynamics of cellular oscillators coupled via contact-mediated interactions. (a) Instantaneous states of oscillator arrays that are (top row) ordered ($\sigma_P = 0$), or (bottom row) disordered to the maximum extent ($\sigma_P = 1$), shown at times separated by an interval that is 1/4 of the oscillation period of an uncoupled cell. Colors represent the expression level of one of the genes (C) comprising the oscillating repressilator circuit [41]. (b), (c) The fraction of realizations f_{ch} in which chimera states are observed (b) and the mean fraction of cells that continue to oscillate $f_{\rm osc}$ (c) shown as a function of the disorder in cellular arrangement (σ_P), as well as the strength of inter-cellular interaction induced repression (measured as $1/Q$). (d), (e) Qualitatively similar behaviors in (d) f_{ch} and (e) $f_{\rm osc}$ are shown by systems of diffusively coupled relaxation oscillators. Increasing the diffusion constant D beyond a critical value leads to cessation of activity through oscillator death. In both systems, increased disorder allows configurations with coexisting oscillating and nonoscillating cells to exist over a much larger range.

Introducing disorder in the cellular arrangement leads to the emergence of chimera states (characterized by the coexistence of oscillating and nonoscillating units) in the collective dynamics [Fig. 3(a)]. As heterogeneity is increased, the range of coupling strengths for which chimera states can be observed increases markedly, appearing even for very weak interactions between cells [Fig. 3(b)]. This is accompanied by cessation of oscillations in the majority of the cells even at low levels of repression [$1/Q \sim 0.01$, see Fig. 3(c)]. Depending on the context, chimeras may have diverse implications, e.g., in growing tissues they potentially contribute to morphogenesis by selective growth, as only the cells that continue to oscillate can keep dividing [22]. Further, in organisms that move via oscillatory beating of ciliary rotors [as in *T. adhaerens*, Fig. 1(b)], chimera states in which certain cilia are rendered immotile can shape the trajectory.

The generality of these results can be demonstrated by using a generic description of relaxation oscillations to describe the dynamical behavior of each cell. This involves a fast activation component u and a relatively slower inactivation (or inhibitory) variable v, whose time-evolution is given by the Fitzhugh-Nagumo equations [47–49]. The lateral inhibition resulting from the receptor-ligand binding mediated interaction mechanism is implemented by diffusive coupling via v between the oscillators [50,51], viz.,

$$du_i/dt = u_i(1-u_i)(u_i-\phi) - v_i, \tag{4}$$

$$dv_i/dt = \epsilon(\kappa u - v - b) + D\,\Sigma_j A_{ij}(v_j - v_i), \tag{5}$$

where $\mathbf{A}$ is the weighted adjacency matrix. The parameters $\phi(=0.139)$, $b(=0.17)$, and $\kappa(=0.6)$ specify the kinetics, and $\epsilon(=0.001)$ is the recovery rate. The strength of diffusive coupling D between neighboring oscillators is analogous to the parameter $1/Q$ for the system of coupled repressilators. Note that increasing disorder in the cellular arrangement alters the diffusive flux between coupled cells, which is proportional to the length l_c of the corresponding interface. This is consistent with l_c being proportional to the density of gap junctions (or other structures that bridge the cytoplasms of cells), provided that they are homogeneously distributed. Figure 3(d) shows that, as in the case of Notch coupled repressilators, increasing heterogeneity promotes the existence of chimera states over a range of D [41]. They can be characterized by the fraction of oscillating cells $f_{\rm osc}$ lying between 0 and 1, with the chimera region straddling the boundary separating global synchronization ($f_{\rm osc} = 1$) from complete quiescence ($f_{\rm osc} = 0$) [Fig. 3(e)]. We have verified that the qualitative features of the transition remain invariant to stochastic fluctuations in molecular concentrations [41]. Thus, disorder-driven transitions appear to be a general phenomenon that might be observed in systems with different mechanisms for oscillations and diverse types of intercellular interactions.

To conclude, we have shown that changes in the packing arrangement of cells, as they become more heterogeneous, modulate their collective behavior arising from intercellular interactions implementing lateral inhibition. This can play a key role in determining the relative proportions of specialized cells, such as neurons [52] or *Drosophila* cells expressing thoracic bristles [25,53]. Furthermore, disorder contributes to tissue robustness against cell damage. The promotion of chimera states upon increasing tissue heterogeneity has multiple implications, including the possibility of selectively regulating growth in confluent tissue or establishing left-right asymmetry by altering large-scale ciliary movement during development [54]. Our results can be experimentally corroborated in epithelial tissue characterized by varying degrees of disorder. For example, *T. adhaerens,* whose cells can continually alter their shape [29,55], could provide a testbed for relating disordered tissue configurations with the collective motion of the cilia attached to every cell. Biofilms comprising oscillating bacterial cells that coordinate their activity by electrical signaling are another potential experimental system to explore how disorder alters collective dynamics [56,57]. Our work suggests a potential role of disorder, which arises during development via cellular remodeling, in shaping morphogenesis.

S.N.M. has been supported by the IMSc Complex Systems Project (12th Plan), and the Center of Excellence in Complex Systems and Data Science, both funded by the Department of Atomic Energy, Government of India. The simulations required for this work were supported by IMSc High Performance Computing facility (Nandadevi).

[1] H. M. Jaeger and S. R. Nagel, Science **255**, 1523 (1992).
[2] H. M. Jaeger, S. R. Nagel, and R. P. Behringer, Rev. Mod. Phys. **68**, 1259 (1996).
[3] W. T. Gibson and M. C. Gibson, Curr. Top. Dev. Biol. **89**, 87 (2009).
[4] P. Formosa-Jordan, M. Ibañes, S. Ares, and J. M. Frade, Development **139**, 2321 (2012).
[5] A. Bottinelli, D. T. J. Sumpter, and J. L. Silverberg, Phys. Rev. Lett. **117**, 228301 (2016).
[6] X. Trepat and E. Sahai, Nat. Phys. **14**, 671 (2018).
[7] A. Kulkarni, S. P. Thampi, and M. V. Panchagnula, Phys. Rev. Lett. **122**, 048002 (2019)
[8] T. Lecuit and P.-F. Lenne, Nat. Rev. Mol. Cell Biol. **8**, 633 (2007).
[9] G. B. Blanchard, A. J. Kabla, N. L. Schultz, L. C. Butler, B. Sanson, N. Gorfinkiel, L. Mahadevan, and R. J. Adams, Nat. Methods **6**, 458 (2009).
[10] F. Jülicher and S. Eaton, Semin. Cell Dev. Biol. **67**, 103 (2017).
[11] K. Molnar and M. Labouesse, Open Biol. **11**, rsob.210006 (2021).
[12] J. A. Zallen and R. Zallen, J. Phys.: Condens. Matter **16**, S5073 (2004).
[13] S. Hilgenfeldt, S. Erisken, and R. W. Carthew, Proc. Natl. Acad. Sci. USA **105**, 907 (2008).
[14] K. Ragkousi and M. C. Gibson, J. Cell Biol. **207**, 181 (2014).
[15] S. Artavanis-Tsakonas, K. Matsuno, and M. E. Fortini, Science **268**, 225 (1995).
[16] R. Kopan and M. X. G. Ilagan, Cell **137**, 216 (2009).
[17] D. Sprinzak, A. Lakhanpal, L. LeBon, J. Garcia-Ojalvo, and M. B. Elowitz, PLoS Comput. Biol. **7**, e1002069 (2011).
[18] O. Barad, D. Rosin, E. Hornstein, and N. Barkai, Sci. Signal. **3**, ra51 (2010).
[19] D. Sprinzak, A. Lakhanpal, L. LeBon, L. A. Santat, M. E. Fontes, G. A. Anderson, J. Garcia-Ojalvo, and M. B. Elowitz, Nature (London) **465**, 86 (2010).
[20] H. Meinhardt and A. Gierer, J. Cell Sci. **15**, 321 (1974).
[21] L. Wolpert and C. Tickle, *Developmental Biology* (Oxford University Press, Oxford, 2011).
[22] C. Kuyyamudi, S. N. Menon, F. Casares, and S. Sinha, Phys. Rev. E **104**, L052401 (2021).
[23] B. Fritzsch, N. Pan, I. Jahan, J. S. Duncan, B. J. Kopecky, K. L. Elliott, J. Kersigo, and T. Yang, Evol. Dev. **15**, 63 (2013).
[24] R. Goodyear and G. Richardson, J. Neurosci. **17**, 6289 (1997).
[25] P. Simpson, Development **109**, 509 (1990).
[26] D. M. Abrams and S. H. Strogatz, Phys. Rev. Lett. **93**, 174102 (2004).
[27] R. Singh, S. Dasgupta, and S. Sinha, Europhys. Lett. **95**, 10004 (2011).
[28] S. Kim, M. Pochitaloff, G. A. Stooke-Vaughan, and O. Campàs, Nat. Phys. **17**, 859 (2021).
[29] V. N. Prakash, M. S. Bull, and M. Prakash, Nat. Phys. **17**, 504 (2021).
[30] K. Grell and A. P. Ruthmann, in *Microscopic Anatomy of Invertebrates, Placozoa, Porifera, Cnidaria and Ctenophora*, edited by F. W. Harrison and J. A. Westfall (Wiley, New York, NY, 1991), p. 13.
[31] C. L. Smith, N. Pivovarova, and T. S. Reese, PLoS One **10**, e0136098 (2015).
[32] G. Buzsáki and A. Draguhn, Science **304**, 1926 (2004).
[33] P. Lenz and L. Søgaard-Andersen, Nat. Rev. Microbiol. **9**, 565 (2011).
[34] L. Potvin-Trottier, N. D. Lord, G. Vinnicombe, and J. Paulsson, Nature (London) **538**, 514 (2016).
[35] M. Guzzo, S. M. Murray, E. Martineau, S. Lhospice, G. Baronian, L. My, Y. Zhang, L. Espinosa, R. Vincentelli, B. P. Bratton, J. W. Shaevitz, V. Molle, M. Howard, and T. Mignot, Nat. Microbiol. **3**, 948 (2018).
[36] A. Ruthmann, G. Behrendt, and R. Wahl, Zoomorphology **106**, 115 (1986).
[37] C. L. Smith, F. Varoqueaux, M. Kittelmann, R. N. Azzam, B. Cooper, C. A. Winters, M. Eitel, D. Fasshauer, and T. S. Reese, Curr. Biol. **24**, 1565 (2014).
[38] M. S. Bull, V. N. Prakash, and M. Prakash, arXiv:2107.02934.
[39] J. Negrete and A. C. Oates, Phys. Rev. E **99**, 042417 (2019).
[40] J. M. Sancho and M. Ibañes, Phys. Rev. E **102**, 032404 (2020).
[41] See Supplemental Material at http://link.aps.org/supplemental/10.1103/PhysRevE.106.L022401 for details, including movies showing the time-evolution of the dynamics in the arrays.
[42] J. Lewis, Curr. Biol. **13**, 1398 (2003).
[43] C. Kuyyamudi, S. N. Menon, and S. Sinha, Phys. Biol. **19**, 016001 (2022).
[44] W.-M. Deng, C. Althauser, and H. Ruohola-Baker, Development **128**, 4737 (2001).
[45] H. Shimojo, T. Ohtsuka, and R. Kageyama, Neuron **58**, 52 (2008).
[46] M. B. Elowitz and S. Leibler, Nature (London) **403**, 335 (2000).
[47] R. FitzHugh, Biophys. J. **1**, 445 (1961).
[48] J. Nagumo, S. Arimoto, and S. Yoshizawa, Proc. IRE **50**, 2061 (1962).
[49] S. Sinha and S. Sridhar, *Patterns in Excitable Media* (CRC Press, Boca Raton, FL, 2015).
[50] R. Singh and S. Sinha, Phys. Rev. E **87**, 012907 (2013).
[51] R. Janaki, S. N. Menon, R. Singh, and S. Sinha, Phys. Rev. E **99**, 052216 (2019).
[52] R. Kageyama, T. Ohtsuka, H. Shimojo, and I. Imayoshi, Nat. Neurosci. **11**, 1247 (2008).
[53] P. Heitzler and P. Simpson, Cell **64**, 1083 (1991).
[54] S. Nonaka, Y. T. Y. Okada, S. T. A. Harada, Y. Kanai, M. Kido, and N. Hirokawa, Cell **95**, 829 (1998).
[55] V. B. Pearse and O. Voigt, Integr. Comp. Biol. **47**, 677 (2007).
[56] A. Prindle, J. Liu, M. Asally, S. Ly, J. Garcia-Ojalvo, and G. M. Süel, Nature (London) **527**, 59 (2015).
[57] J. Humphries, L. Xiong, J. Liu, A. Prindle, F. Yuan, H. A. Arjes, L. Tsimring, and G. M. Süel, Cell **168**, 200 (2017).